Cardiovasc Toxicol (2007) 7:215–234
DOI 10.1007/s12012-007-9003-x

Deterministic and Stochastic Models of NFκB Pathway

Tomasz Lipniacki · Marek Kimmel

Published online: 18 October 2007
© Humana Press Inc. 2007

Abstract In the article, we discuss the state of art and perspectives in deterministic and stochastic models of NFκB regulatory module. The NFκB is a transcription factor controlling various immune responses including inflammation and apoptosis. It is tightly regulated by at least two negative feedback loops involving IκBα and A20. This mode of regulation results in nucleus-to-cytoplasm oscillations in NFκB localization, which induce subsequent waves of NFκB responsive genes. Single cell experiments carried by several groups provided comprehensive evidence that stochastic effects play an important role in NFκB regulation. From modeling point of view, living cells might be considered noisy or stochastic biochemical reactors. In eukaryotic cells, in which the number of protein or mRNA molecules is relatively large, stochastic effects primarily originate in regulation of gene activity. Transcriptional activity of a gene can be initiated by transactivator molecules binding to the specific regulatory site(s) in the target gene. The stochastic event of gene activation is amplified by transcription and translation, since it results in a burst of mRNA molecules, and each copy of mRNA then serves as a template for numerous protein molecules. Another potential source of variability can be receptors activation. At low-dose stimulation, important in cell-to-cell signaling, the number of active receptors can be low enough to introduce substantial noise to downstream signaling. Stochastic modeling confirms the large variability in cell responses and shows that no cell behaves like an "average" cell. This high cell-to-cell variability can be one of the weapons of the immune defense. Such non-deterministic defense may be harder to overcome by relatively simple programs coded in viruses and other pathogens.

Keywords Mathematical modeling · Systems biology · Immune response · NFκB · Stochastic regulation · Stochastic robustness · Single cell

T. Lipniacki (✉)
Polish Academy of Sciences, Institute of Fundamental Technological Research, Swietokrzyska 21, 00-049 Warsaw, Poland
e-mails: tomek@rice.edu; tlipnia@ippt.gov.pl

T. Lipniacki · M. Kimmel
Department of Statistics, Rice University, 6100 Main St., MS-138, Houston, TX 77005, USA

M. Kimmel
Systems Engineering Group, Silesian Technical University, Akademicka 16, 44-100 Gliwice, Poland

Introduction

There are two main ways in which mathematics interacts with biology. The first leads indirectly through physics and chemistry. Since mathematics is proved to be an efficient language of physics, and quantum physics is the basis for modern chemistry, this approach appears natural and sound. The idea that biology might be reduced to physics is at least as old as quantum physics and was supported by outstanding physicists, such as Bohr and Schrödinger. This idea seems to be not as widely supported by biologists as it is by some mathematicians and physicists. Despite a controversy, most scientists on either side will agree that biology may be reduced to physics in the sense that biological processes follow, or are not contradictory to, physical laws. However, this does not mean that one can solve biological problems, like kinetics of cell cycle, by solving the Schrödinger equation. In fact, we cannot even perform a complete numerical simulation of protein

folding, and therefore, from the physical standpoint, we cannot determine the protein function based on the amino acid sequence. This latter problem may be possibly overcome by application of faster computers. Nevertheless, it appears naive to expect that we may ever have enough computing power to solve the cell evolution based purely on physical laws.

This impossibility justifies the existence of mathematical biology. Mathematical biology starts from elementary biological experimental findings in order to make the more complex predictions. In the area of molecular biology the experimental finding may have a form of matrix M_1 of interactions between a set of proteins P_i or of matrix M_2 of interactions between transcription factors F_i and genes G_i. We may determine the second matrix by microarray experiments, but in most cases we may not predict by pure physical considerations that the transcription factor F_i binds stably to the promotor region of gene G_i. Although from the physical standpoint, this is not the solution, we may build a mathematical model based on experimental knowledge collected in matrices M_1 and M_2 and make useful predictions about the behavior of the regulatory pathway involving the components. Obviously mathematical modeling may not contradict physical laws, but it may not necessarily be based on physical reasoning. The gaps, too difficult to be solved by physical calculations, can be filled by experimental knowledge.

We should keep in mind that the status of mathematical modelling in biology is weaker than in physics or chemistry. In physics there are a few elementary laws, and mathematics used to derive more complex relations from the elementary laws. In mathematical biology, we do not start from elementary laws, and typically we do not have enough data to make our models unique. There always exists the risk that new experiments will contradict our predictions. One might only hope that rapidly developing experimental techniques, allowing quantitative description of processes at molecular level, together with steadily improving computational methods, will bring biophysics and mathematical biology closer. This should result in more accurate physical–mathematical models of biological processes.

Modeling of regulatory networks typically starts from cartoons summarizing preliminary knowledge, in which the potentially important interactions between the components are depicted by "suppressing" or "activating" arrows. Such cartoons may relatively simply describe very complicated metabolic or regulatory networks. However, to allow quantitative analysis, they must be transformed into mathematical models in which arrows are replaced by differential equations in a deterministic description or by particle–particle interactions in a stochastic description.

Most regulatory network models are based on the assumption that the reacting substrates are well-mixed in the cell nucleus and in the cytoplasm and consider only transport between but not within these two compartments. This assumption, when used in modeling of single cells, expresses lack of knowledge of spatial distribution of cell components. However, this set up is also commonly used in modeling of cell populations, as if cell populations could be represented by aggregate nucleus and aggregate cytoplasm, with boundaries of cells dissolved. For this, the only justification is practical usefulness.

Deterministic modeling hinges upon the assumption that the number of reacting particles is fairly large, so the chemical reactions between the components might be modeled using ordinary differential equations (ODEs) based on mass action law. In bacteria such approximation is poorly justified since typically the number of mRNA transcripts and proteins is very low. Mammalian cells are about three orders of magnitude larger than bacteria, so the deterministic approximation is much better justified. However, even in this case, some reactions such as mRNA transcription involve very small numbers of molecules (two DNA copies), which limits the accuracy of the mass action formulas.

As noted above, ordinary differential equations sometimes are considered adequate to describe cell population models, i.e., models which predict the average behavior in the population. However, the average behavior may be very different from the behavior of any cell in the population. If, for example, half of cells in the population choose proliferation pathway and the other half the apoptotic pathway, then the average will not correspond to any biological process.

The most accurate tool of modeling of single cells, involving low-molecule number effects, is the Gillespie stochastic simulation algorithm [1]. This algorithm is widely applied for regulatory networks in bacteria, however, in mammalian cells, in which the number of reacting proteins may be of order of 10^5, it becomes numerically inefficient.

There are several way to speed up the Gillespie algorithm. The simple and natural one, proposed by Haseltine and Rawlings [2], splits the reaction channels into fast and slow. Fast reactions are described by the deterministic-rate equations, while the slow reactions are considered stochastic. This approach typically speeds up simulations by several orders of magnitude. This advantage may become less important in nearest future due to growing numerical capabilities, which might allow direct Monte Carlo simulations of large networks. The other advantage of splitting reactions into slow and fast is that it helps to identify "switching points" in a regulatory network. At such points, the stochastic effects dominate and may control the fate of

individual cells in population. Detailed analysis of these switching points is crucial for understanding of the whole pathway.

The aim of the present review is to discuss general issues of deterministic and stochastic modeling of regulatory and signaling pathways with a special focus on recent developments on NFκB signaling. Nuclear factor κB (NFκB) regulates numerous genes important for pathogen or cytokine inflammation, immune response, cell proliferation and survival (reviewed by Brasier [3] and Hoffmann and Baltimore [4]). In mammals, the NFκB family of transcription factors contains five members but the ubiquitously expressed p50 and RelA heterodimer is responsible for the most common inducible NFκB binding activity. In resting cells, p50|RelA heterodimers referred herein to as NFκB are sequestered in the cytoplasm by dimerization with members of another family of proteins called IκB. This family includes several proteins, but most of the IκB-family inhibitory potential is carried by IκBα, whose synthesis is controlled by a highly NFκB-responsive promoter, resulting in autoregulation of NFκB signaling [5]. Activation of NFκB requires degradation of IκBα, which allows NFκB to translocate into the nucleus, bind to κB motifs present in promoters of numerous genes and upregulate their transcription. NFκB activating signals converge on the cytoplasmic IκB kinase (IKK), a multiprotein complex that phosphorylates IκBα leading to its ubiquitination and then to its rapid degradation by the proteasome. Activation of IKK kinase is induced by various extracellular signals including tumor necrosis factor-alpha (TNFα), interleukin-1 (IL-1) and lipopolysaccharide (LPS) through complicated, not fully resolved, transduction pathways. IKK inactivation is controlled by the zinc finger protein termed A20, the transcription of which, like that of IκBα, is strongly NFκB responsive and generates a second negative feedback loop in NFκB signaling [6]. Mice deficient in A20 develop severe inflammation and cachexia, are hypersensitive to TNF, and die prematurely [7].

The article is organized as follows; first we discuss background issues of NFκB models, then we review existing deterministic and stochastic models and conclude with discussion and further perspectives.

Background on NFκB Pathway Models

Immune response is regulated by a number of interconnected regulatory and signaling pathways, see [8] for recent review. These pathways have some features in common and their modeling encounters common problems. Signaling pathway involves several distinct stages and process: Accommodation of extracellular or intracellular signals (receptors), amplification of the signal (transduction pathways), transport between nucleus and cytoplasm, gene regulation, mRNA transcription, and protein translation. The core of the pathway is typically the regulatory module, which involves feedback or feedforward loops. In the case of NFκB this core is formed by the IκBα–NFκB signaling module. The inhibitory protein IκBα suppresses NFκB transcriptional activity by binding to NFκB molecules and keeping them inactive in the cytoplasm. In turn, NFκB positively regulates IκBα transcription by binding the IκBα promoter. The module is driven by activated IKK kinase, which phosphorylates IκBα, which leads to its ubiquitination and then to its rapid degradation by the proteasome (reviewed in [9]). Activity of IKK kinase results from various stimulations, and is attenuated by another NFκB-responsive protein A20, which provides the second negative feedback loop. In Fig. 1, we present the schematic NFκB regulatory pathway based on models by Hoffmann and coworkers [10, 11], Lipniacki et al. [12] and Park et al. [13]. The core may be stimulated by various signals like TNFα, IL-1, LPS, and viruses or other pathogens, which converge at the level of IKK. The output signals stream from the core by means of over 100 gene products, whose transcription is regulated or coregulated by NFκB. There are at least three classes of NFκB regulated genes expression of which peaks at about 1, 3, and 6 h of continuous NFκB stimulation. Two NFκB inhibitors IκBα and A20, as well as inflammation controlling interleukines belong to the first group of early genes, which may be upregulated even by a short 5-min pulse of TNFα stimulation. The later genes require prolonged stimulation. In the first approximation the feedback-regulated core can be understood as an input–output box, which transforms the external signal to pulses of active nuclear NFκB.

The common building blocks of deterministic models are ODEs based on the mass action law, supplemented by cytoplasm–nucleus exchange ODEs. In many cases, the fast catalytic reactions are modeled by Michaelis–Menten formulas which allows reducing the number of equations. In modeling of the NFκB pathway, the key processes are

- mRNA transcription and protein translation of NFκB inhibitory proteins: IκBα (and other IκB isoforms) and A20;
- inter compartment transport of IκBα, NFκB and their complexes;
- formation of protein complexes;
- catalytic activation of IKK;
- catalytic degradation of IκBα (and other IκB isoforms) due to IKK-induced phosphorylation and subsequent ubiquitination.

In stochastic modeling the same reactions are considered, but part or all of them they are simulated by stochastic algorithms. As already said the exact method is

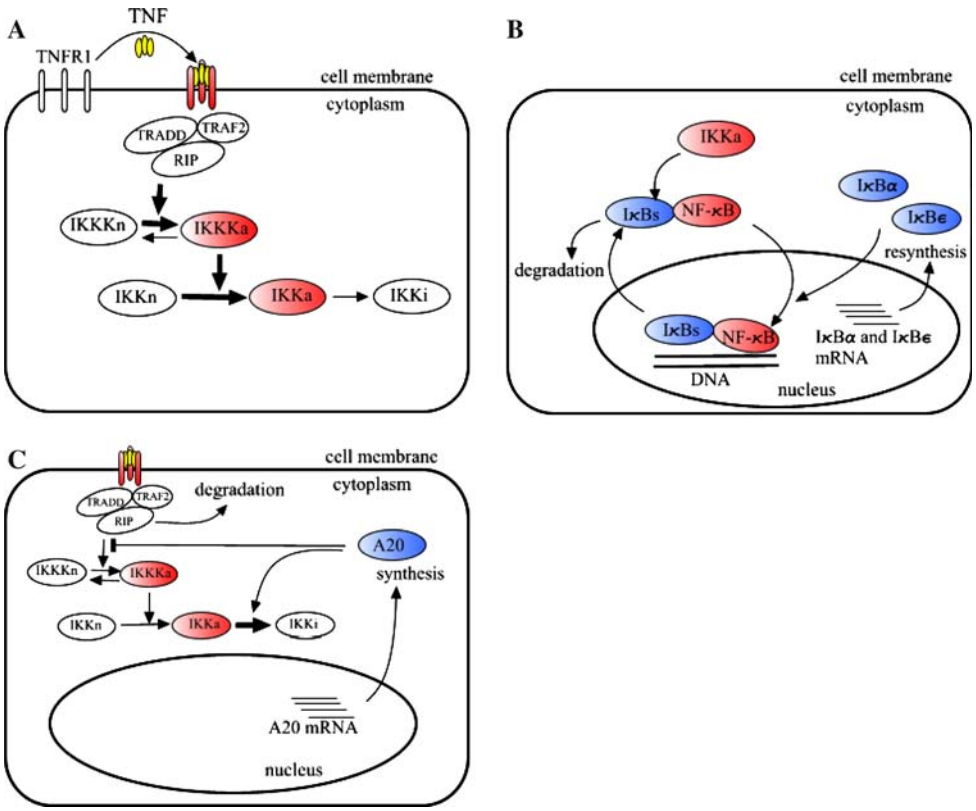

Fig. 1 Schematic of the NFκB regulatory pathway activated by TNFα, including the features of Hoffmann et al. [10, 11], Lipniacki et al. [12], Park et al. [13] models. (**a**) TNFR1 receptor activation and signal transduction. Ligand binding leads to trimerization of the TNFR1 receptor. Formation of the active receptor complex involves binding of the several proteins including TRADD, TRAF2, and RIP. Active receptor activates the IKKK (IKK kinase) transforming it from the neutral IKKKn to the active form IKKKa. In turn IKKKa activates IKK by transforming it to the active state IKKa, in which it is capable of phosphorylating the IκB proteins (IκBα, IκBε, IκBβ). (**b**) NFκB|IκBα/IκBε autoregulatory loop. NFκB is found in an inactivated complex in the cytoplasm with its inhibitor IκBα. IKKa, phosphorylates and degrades both free and NFκB complexed IκBs. Liberated NFκB enters the nucleus to induce transcription of IκBα, IκBε and A20 genes. The IκBα protein is rapidly resynthesized, enters the nucleus and recaptures NFκB back into the cytoplasm. The IκBε protein is also degraded due to IKKa-induced phosphorylation and then resynthesized [11] but at slower rate than IκBα. However, in the continued presence of IKKa, the resynthesized IκBα/IκBε are continuously degraded, resulting in a continued nuclear NFκB translocation. (**c**) The NFκB-A20 autoregulatory loop. A second level of negative autoregulation occurs with the synthesis of A20. A20 is an ubiquitin ligase that degrades signaling intermediates coupling the TNFα receptor with continuous IKK activation, and directly associates itself with IKKa, converting it to the catalytically inactive IKKi. It leads also to RIP ubiquitination and degradation attenuating receptors activity

the Gillespie algorithm in which all the reaction are considered stochastic. We highlight the approximate approach in which only reactions involving gene activation and inactivation are modelled as stochastic, while the rest of reactions involving transcripts and proteins are modeled by ODEs.

Modeling Stochastic Gene Expression

Stochasticity in gene expression may arise from fluctuation in gene activity [14], mRNA transcription, protein translation and oligomerization [15–18], reviewed recently in [19]. Figure 2 illustrates the main steps in gene expression. Control of gene activity is mediated by transcription factors which may bind to the specific promoter regions and switch the gene *on* or *off*. When the gene is active, RNA polymerase may bind to the gene promoter and initiate mRNA transcription. Next, mRNA is edited and exported from the nucleus to the cytoplasm, where the protein translation occurs. Accordingly, a single event of gene activation results (if the activation period is sufficiently long) in a burst of mRNA molecules, which is then translated into an even larger burst of proteins [14, 20, 21]. Stochasticity in gene expression causes that the population of cells exhibits a large cell-to-cell variability, as observed for example, by Takasuka et al. [22] and Stirland et al. [23], for mammalian cells, Raser and O'Shea [24], for budding yeast (*Saccharomyces cereviciae*) or Elowitz et al. [25], for bacteria (*Escherichia coli*).

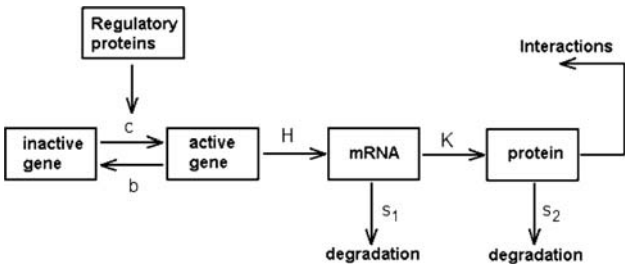

Fig. 2 Simplified schematic diagram of gene expression

Let us consider a single haploid gene, expression of which is controlled by regulatory factors F_i. These can be transcription factors which promote mRNA polymerase binding and thus transcription or repressors which switch the gene off. The simplified model depicted in Fig. 2 involves three classes of processes, namely; gene activation/inactivation, mRNA transcription/decay, and protein translation/decay. It is assumed that the gene can be transformed into the active state denoted by A with a propensity (rate) $c(F_i)$, and transformed into inactive state denoted by I with propensity $b(F_i)$, due to binding and dissociation of regulatory factors, respectively. We further assume that mRNA transcript molecules are synthesized at a rate $G(t)H$, where G is a binary variable describing the state of a gene: $G(A) = 1$ and $G(I) = 0$ [14, 26–28]. Protein translation proceeds at a rate $Kx(t)$, where $x(t)$ is the number of mRNA molecules. In addition mRNA and protein molecules are degraded at rates s_1 and s_2, respectively. The reactions described can be summarized as follows:

$$I \xrightarrow{c(F_i)} A, \quad I \xrightarrow{b(F_i)} A, \tag{1}$$

$$A \xrightarrow{GH} \text{mRNA} \xrightarrow{s_1} \phi, \tag{2}$$

$$\text{mRNA} \xrightarrow{K} \text{protein} \xrightarrow{s_2} \phi, \tag{3}$$

where the degradation of gene products is represented by symbol ϕ. The resulting protein may then form complexes with other proteins, may translocate between cytoplasm and nucleus, and eventually may be itself the regulatory protein for other genes or for its own gene.

The state of the system is given by the triple $(x(t), y(t), G(t))$, where $y(t)$ is the number of protein molecules. It the case when the transition coefficients c and b are constant, equations (1–3) describe the so-called Markov process, i.e., the process without memory, for which the propensity function of the transition from state $(x(t), y(t), G(t))$ to the state $(x'(t+\Delta t), y'(t+\Delta t), G'(t+\Delta t))$ depends solely on the triple (x, y, G). In the case, when functions $c(F_i)$ and $b(F_i)$ are not constant, in order to make the system Markovian, one must include the processes governing the evolution of F_i. Unfortunately, in most cases the evolution of regulatory proteins F_i will depend to the other proteins or protein complexes. Finally, we may end up on the system describing the evolution of the whole cell, which again is Markovian only if we neglect the extracellular influence. The are two exact methods to analyze evolution of the Markovian systems. The most straightforward is direct simulation using the Gillespie algorithm [1]. In this method, for a given state of the our system (x, y, G) the propensity r_i of each possible reaction, such as the change of a gene state, synthesis of mRNA or protein and degradation of mRNA or protein, is determined. The total propensity function is $r = \sum r_i$. Now, we randomly chose two numbers p_1 and p_2 from the uniform distribution on (0,1). The first number is used to calculate time $t = -\ln(p_1)/r$ at which the nearest reaction occurs. The second number yields the index k of the nearest reaction that occurs, based on the condition

$$\sum_{i=1}^{k-1} r_i < p_2 r \leq \sum_{i=1}^{k} r_i. \tag{4}$$

The other method is to compute a pair of probability mass functions:

$$f_{xy} = P[\#\,\text{mRNA} = x, \#\,\text{protein} = y, G = 0], \tag{5}$$

$$g_{xy} = P[\#\,\text{mRNA} = x, \#\,\text{protein} = y, G = 1], \tag{6}$$

which constitute the joint probability that the number of mRNA molecules (of considered species) is equal to x and the number of protein molecules is equal to y, and the cell is in the inactive ($G = 0$) or active ($G = 1$) state.

Time evolution of the distribution (5–6) is given by the following system of chemical master equations [26, 29],

$$\begin{aligned}\frac{df_{xy}}{dt} &= bg_{xy} - cf_{xy} + G(I)Hf_{x-1,y} + s_1(x+1)f_{x+1,y} \\ &\quad - (G(I)H + s_1x)f_{xy} + Kxf_{x,y-1} + s_2(y+1)f_{x,y+1} \\ &\quad - (Kx + s_2y)f_{xy},\end{aligned} \tag{7}$$

$$\begin{aligned}\frac{dg_{xy}}{dt} &= -bg_{xy} + cf_{xy} + G(A)Hg_{x-1,y} + s_1(x+1)g_{x+1,y} \\ &\quad - (G(A)H + s_1x)g_{xy} + Kxg_{x,y-1} + s_2(y+1)g_{x,y+1} \\ &\quad - (Kx + s_2y)g_{xy}.\end{aligned} \tag{8}$$

Since $x \in \mathbb{N}$ and $y \in \mathbb{N}$, the above is an infinite system of equations. The first two terms in Eqs. (7 and 8) correspond to the time change of probability, due to the regulation of gene activity, next three terms correspond to the time change of the probability due to the synthesis/degradation mRNA molecules, while the last three terms correspond to the synthesis/degradation of protein molecules. Note that since $G(I) = 0$, the mRNA synthesis terms are absent in Eq. 7. The master equations (7 and 8) describe exactly the time-dependent distribution of the

underlying stochastic process, and thus their solution is of primary interest. Although these equations may not be solved analytically even for constant c and b, they can be used to calculate the moments of distributions f_{xy}, g_{xy}.

As already said the two described approaches can be applied to more complicated systems of arbitrary number of genes expressing interacting proteins. However, they become computationally very inefficient, when the number of interacting molecules is large.

In recent years several approximate methods were proposed that accelerate the Gillespie algorithm. One is the τ-leap method [30, 31], in which time is divided into intervals of length τ. It is required that τ be short enough so that the propensity functions for all reactions remain almost unchanged. Assuming that this is satisfied, the number of reactions in each reaction channel is a Poisson random variable with parameter equal to the τ-interval propensity for the reaction channel considered.

Another method has been devised by Haseltine and Rawlings for the case, when it is possible to separate the system into slow and fast reaction channels [2, 32]. The idea is to approximate the "fast" reactions either deterministically or using chemical Langevin equations, and to treat the "slow" reactions, as stochastic events with time-varying reaction rates. Langevin equation [29] itself combines deterministic description of evolution of, say, variable x with a stochastic process, typically white noise, $\eta(t)$

$$\frac{dx}{dt} = f(x) + \eta(t) \tag{9}$$

and provides a more accurate description than a deterministic equation. Recently the idea of Haseltine and Rawlings has been improved by Cao et al. [33], who introduced a virtual fast system, being Markovian, which makes the analysis simpler. This improves the analysis in the cases, when fast reactions are described by Langevin equations. In the case in which the fast reactions are fast enough to be described by the deterministic-rate equations, the Cao et al. [33] method is reduced to that of Haseltine and Rawlings [2]. Combining the τ-leap method and Haseltine and Rawlings' idea, Puchalka and Kierzek [34] proposed an approach in which slow reactions are simulated exactly while fast reaction are simulated by τ-leap method.

Assuming that all reactions except these of gene activation and inactivation are fast, we may approximate system (1–3) by the following [28],

$$I \xrightarrow{c(F_i)} A, \quad I \xleftarrow{b(F_i)} A, \tag{10}$$

$$\frac{dx}{dt} = HG(t) - s_1 x, \tag{11}$$

$$\frac{dy}{dt} = Kx - s_2 y. \tag{12}$$

In this approximation, stochasticity related to the synthesis/degradation of mRNA and proteins is neglected. We consider x and y as continuous variables and replace Eqs. 2 and 3 by the deterministic reaction-rate equations. In the next section, we show the implementation of this approach to the NFκB model.

Experiment Versus Modeling

From the modeling perspective there are three classes of experimental data:

- Population measurements, such as Electrophoretic Mobility Shift Assay (EMSA) Western and Northern blots, kinase activity assays, and DNA-microarrays.
- Single cell, single time point measurements, such as flow cytometry and in situ hybridization.
- Single cell evolution experiments, such as experiments with use of fluorescently tagged proteins, and stable and transient transfections.

The main advantage of population measurements in addition to their relative simplicity is that they measure a relatively unperturbed system or the system perturbed in the way we want it to be. The disadvantage is the averaging, which can make single-cell effects invisible.

Single cell, single time point measurements provide information about time dependent distribution. The accuracy of such experiments is typically low but compensated by a large number of cells which can be measured. Time evolution of the distribution does not however contain enough information to deduce single-cell dynamics. For example the fact that the distribution is not time dependent does not imply that single cell trajectories are constant in time. As we will see, at later times from the beginning of the TNFα stimulation, NFκB distribution remains almost constant but all cells oscillate.

The stochastic models considered show that both intrinsic and extrinsic noise can cause population of oscillating cells to become desynchronized. In the case of NFκB regulation, for the first 2–3 h after stimulation most cells remain quite well synchronized, so the population analysis make sense. Later on, the single-cell oscillations are cancelled out by averaging. Therefore, at later time points, data obtained by from population experiments can be very misleading and may lead to wrong models.

In contrast, in single-cells experiments, we may trace single cell evolution but typically the system is strongly perturbed. In transfection experiments the amount of interacting proteins may be substantially increased. Since the regulatory networks are nonlinear, it is naive to expect that evolution of transfected cells will be identical as in wild type cells. In the case of NFκB regulation the increased level of RelA molecules leaves the period of oscillations almost unchanged. This may be due to the fact that even the normal level of RelA is high enough to activate the NFκB dependent genes once NFκB enters the nucleus. The same is not true for IκBα transfection; the increased expression of the inhibitors substantially changes the oscillations [35]. The best solution would be to replace genes of interest by their homologs coding for the fluorescent protein, which is difficult experimentally. Before such experiments are done, the natural but also difficult solution for modelers is to run the model for normal and elevated number of alleles. The model with elevated expression should be then compared to single-cell experiments, and the model with normal number of alleles averaging over many runs with the population data.

In recent years, several important studies of NFκB regulation at the single-cell level have been performed [36–39]. Using fluorescently tagged RelA and IκBα proteins, these experiments enable observation of inter-compartment translocations of both proteins, showing a large heterogeneity in kinetics of cell responses to TNFα or IL-1 stimulation. Nelson et al. [37], showed that the rate of nuclear RelA accumulation in response to TNFα stimulation depends on the initial RelA:IκBα ratio. In cells with enhanced initial concentration of IκBα, the nuclear import is considerably slower. In agreement with Nelson et al. [37], Schooley et al. [39] found a broad distribution of nuclear RelA levels in the cell population at 10–90 min after IL-1 stimulation. Although these experiments indicate a large variability in cell kinetics, it is not straightforward to determine to which extent this variability is caused by stochastic regulation of gene expression, rather than being introduced by cell-to-cell variation in the amount of transfected plasmids (or their expression levels). In a recent experiment, Nelson et al. [35], proved existence of long persisting single-cell oscillations in NFκB signaling. Since cell-to-cell synchronization decreases with time, these oscillations either do not appear or appear strongly damped when observed at the population level, but as concluded by the authors they are important in control of expression of numerous NFκB inducible genes. The point is that NFκB must circulate between nucleus and cytoplasm where it may become activated by a post-translational modification, such as phosphorylation. Inhibition of its nuclear export results both in NFκB dephosphorylation at Ser 536 after about 3 h and in transitory κB-dependent luciferase reporter gene expression that peaks after about 5 h [35].

In order to build reliable models, of paramount importance are experiments, which use various stimulation protocols, such as with pulse and continuous stimulation, pulse–pulse stimulation, knock outs, mutations blocking particular protein functions. Such perturbations are in most cases easy to simulate by the model, and they allow clarifying the role of various components and relations between these components.

Model Fitting

Typically many kinetic parameters are unknown, so the model must be fitted based on experimental data. The problem is far from trivial. The deterministic models are commonly considered as population models and fitted to population data, which have the form of blots, EMSA assay, kinase activity assays, or microarray data. However, if the cells are not synchronized, the model which accurately agrees with population data may not describe any biological process. For example the single-cell experiments and stochastic models suggest that in the case of NFκB regulatory module several hours after TNFα stimulation none of cell behave like the "average cell". This is even more pronounced when one considers the eventual fate of a particular cell, which in the case of TNFα stimulation is either proliferation (survival) or apoptosis.

For a reliable fit, one needs data collected using various simulation protocols for most of model variables. For example, the Hoffmann et al. [10] model was fitted based on data coming from continuous and pulse stimulation (with pulse duration of 5, 15, 30 and 60 min) for wild type cells and cells with various knockouts of IκB isoforms. Lipniacki et al. [12] model was fitted to data with various time protocols and to wild type and A20 deficient cells.

One of methods is "manual" fitting. Its advantage is that it can employ data which are not quantified, the second is that it allows to base the fit on intuitive criteria and information from different researchers. The main disadvantage is that is extremely time-consuming and thus restricted to relatively small systems. The other disadvantage is that the final result is researcher-dependent. In Lipniacki et al. [12] the following fitting method was proposed:

(1) Start from a reasonable set of parameters, which produces a correct steady state for non-stimulated cells.

(2) Proceed with the signal initiated by stimulation along the autoregulatory loops.
(3) Iterate item 2 until the fit to all data is satisfactory.

If there were no feedback loops in the pathway, the proposed method would be quite efficient, but, since they exist, it is necessary to iterate the signal tracing step several times, until the fit is satisfactory. Once a satisfactory fit is found, we observe that the set of parameters chosen to fit the data is by far not unique. This ambiguity is mainly caused by the lack of measurements of absolute values of protein or mRNA amounts. The action exerted by some components of the model on the rest of the pathway is determined by their amounts multiplied by undetermined coupling coefficients. Hence, once we have a good fit, we may obtain another one using a smaller coupling coefficient and by proportionately increasing the absolute level of the component. There also exist single parameters, the value of which can be changed over a very broad range without a significant influence on the time behavior of any substrate or complex for which the data available.

In addition to the time-consuming manual fitting methods there exist several fitting engines. All these methods encounter two major problem: first is data quantification, which is sometimes difficult because of nonlinearities in signal to data transformation. Second is ambiguity in choosing the good fit criteria. The most popular least square criterion can be very misleading for oscillatory trajectories: For example, according to this method, the profile with oscillations with slightly different period may give a worse fit than no oscillations at all. As noted by Mendes [40] the least-square criterion, when applied to oscillatory behavior is biased toward optimizing frequency rather than amplitude and overall qualitative shape of the curve. This is because even a small shift in frequency can lead to a substantial increase in the sum of residuals, see Hoffmann et al. [10] Supplementary Data and Mendes [41] for discussion.

Recently, Fujarewicz et al. [42] discussed the use of reverse-time adjoint dynamical system to accelerate computation of gradients in the steepest descent method. This method was tried with a success on the same data set that was used in [12].

There are still open issues regarding fitting the stochastic models. In the case when stochasticity is only a corollary to deterministic evolution, one may fit the deterministic approximation to population data. However, when stochastic effects dominate the evolution, the population data can be quite misleading and may not be used to fit the single cell trajectories. In such case a well-fitted model should reproduce the average only after averaging over many single cell simulations. It should also reproduce experimentally measured time-dependent covariance of model variables.

Review of Models of the NFκB Module

Deterministic Models

One-feedback Model: Interplay Between IκB Isoforms

The first comprehensive mathematical model of the IκB–NFκB signaling module was proposed by Hoffmann et al. [10] to analyze the interplay between three IκB isoforms. The model describes oscillations in cytoplasm-to-nucleus localization of NFκB upon the TNFα stimulation. These oscillations are due to the negative feedback loop regulation, and time delay. In resting cells NFκB is sequestered in the cytoplasm by association with three IκB isoforms. The feedback regulation is induced by the active IKK, which is assumed to appear immediately after TNFα stimulation and leads to phosphorylation and degradation of IκB. The nuclear translocation of the transcriptional factor NFκB causes induction of synthesis of its principal inhibitor IκBα, which then binds to NFκB and carries it to the cytoplasm. The time delay is due mainly to subsequent processes of IκBα mRNA transcription, IκBα translation and transport to the nucleus. These processes introduce about half-an-hour gap between IκBα induction and NFκB repression.

Oscillation damping is controlled by action of two other members of IκB family: IκBβ and IκBε, which also inhibit NFκB by sequestering it in the cytoplasm, but are not NFκB responsive. It is assumed that the mRNA transcription efficiency of IκBβ and IκBε is constant, while that of the IκBα is a sum of constant term and a term proportional to the square of the nuclear concentration of NFκB. The model shows that the oscillation damping decreases with decreasing magnitude of transcription speed of IκBβ and IκBε genes, eventually without any IκBβ and IκBε expression the oscillations are almost undamped. This is confirmed by experiment in which the knockout of IκBβ and IκBε genes substantially lowers the oscillation damping. The experiment also shows that the knockout of IκBα and any of IκBβ and IκBε genes causes the cells no longer to exhibit any oscillations, Fig. 3. In this case NFκ B enters the nucleus and remains there at almost unchanged level for 6 h. Interestingly, it takes more time for NFκB to enter the nucleus in the case when IκBα gene is knocked out. This shows the higher stability of IκBβ and IκBε proteins, which bind NFκB in the absence of IκBα. The behavior of the system upon the knockout of IκBα and any of IκBβ and IκBε genes is well predicted by the model, however, it is necessary to increase 7-fold the transcription rate of IκBβ and IκBε genes compared to that assumed to fit the experiment without any knockout. This, as stated by the authors, suggests some crossregulation between IκB isoforms. It may also imply that IκBβ and IκBε are to some

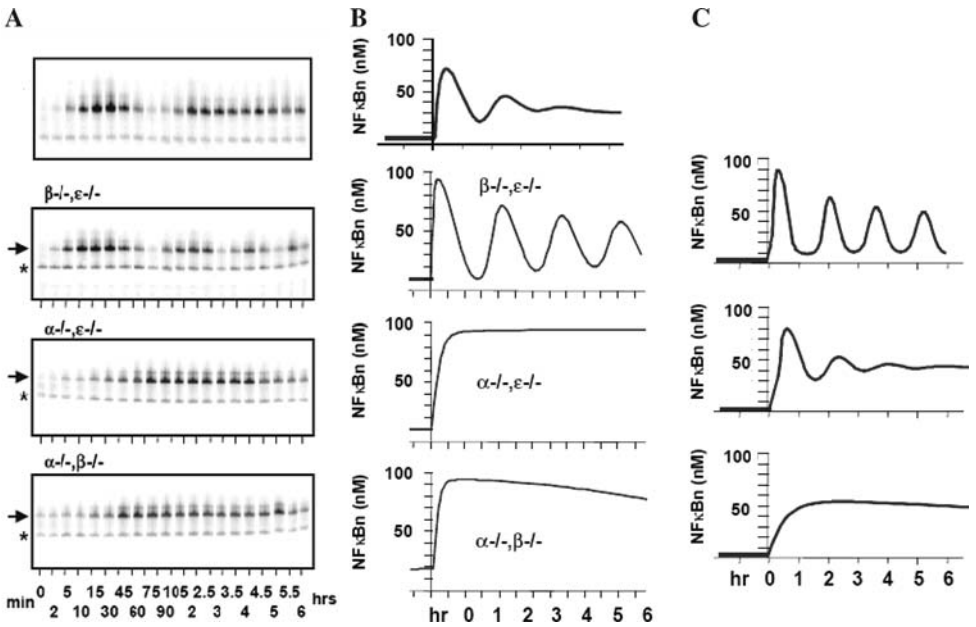

Fig. 3 Hoffmann et al. [10] model describing genetically reduced systems. (**a**) Analysis of NFκB$_n$ by EMSAs of nuclear extracts prepared at indicated times after stimulation fibroblasts with the indicated genotype and wild type cells with TNFα (10 ng/ml). Arrows indicate specific nuclear NFκB binding activity; asterisks indicate nonspecific DNA binding complexes. (**b**) Computational modeling of indicated genotypes. (**c**) Models of the signaling module, with increasing IκBβ and IκBε constitutive transcription rates, keeping the IκBα transcription rate constant. mRNA constitutive synthesis for IκBβ and IκBε are increased fivefold (top to middle) and then sevenfold (middle to bottom). The bottom panel represents the NFκB$_n$ output predicted by a model with mRNA synthesis parameters identical to those employed in the single IκB isoform models of (**b**)

extent NFκB responsive, in fact recently Kaerns et al. [11] found that IκBε is the NFκB responsive, and it provides negative feedback to control NF-κB oscillations. In this case, the knockout of IκBα, increasing the level of nuclear NFκB in resting cells, will result in higher expression of IκBβ and IκBε genes.

The mathematical representation of the model consists of 23 ordinary differential equations (see [10] Supplementary data) accounting for:

I. Transport between compartments: all IκB isoforms and NFκB as well as IκB|NFκB complexes may exits in cytoplasm and nucleus and their translocations are key to the regulation. It is assumed that free NFκB quickly translocates to the nucleus while IκB|NFκB complexes translocate to the cytoplasm. Free IκB isoforms migrate between two compartments. IKK is assumed to be purely cytoplasmic.
II. Spontaneous degradation of IκB mRNA and proteins, and active degradation of IκB proteins due to phosphorylation by the active IKK.
III. Formation of protein complexes, dimers IκB|NFκB and Iκ B/IKK, and trimers IκB|NFκB|IKK.
IV. mRNA transcription of κB isoforms: as already stated, it is assumed that the transcription efficiency of IκBβ and IκBε is constant while the IκBα is a sum of constant term and the term proportional to the square of the nuclear concentration of NFκB.

The model describes the core of NFκB signaling module, i.e., the IκBα–NFκB negative feedback loop, together with IκBβ and IκBε dampers. In last 4 years the model was modified and used by various groups of researchers.

Further Work Expanding Hoffmann et al. Model

After Hoffmann et al. [10] model had been published, Werner et al. [43] compared TNFα and LPS induced NFκB activation, see Fig. 4. TNFα stimulation results in a sharp narrow peak of IKK activity at about 10 min of stimulation, followed by low tail. In the case of LPS stimulation Werner et al. [43] found that the IKK activity gradually grows due to the positive feedback loop controlled by NFκB and IRF3 (interferon-regulatory factor 3) and resulting in the TNFα synthesis, which in turn activates the TNFα receptors. As a result the IKK activity peaks at 60 min and remains at a high level for the next hour. The authors took as an input the experimentally determined IKK profile and then calculates the evolution of the downstream pathway, with the aid of Hoffmann et al. [10] model. In this version of the model an even higher cooperativity is assumed in NFκB binding; the transcriptional

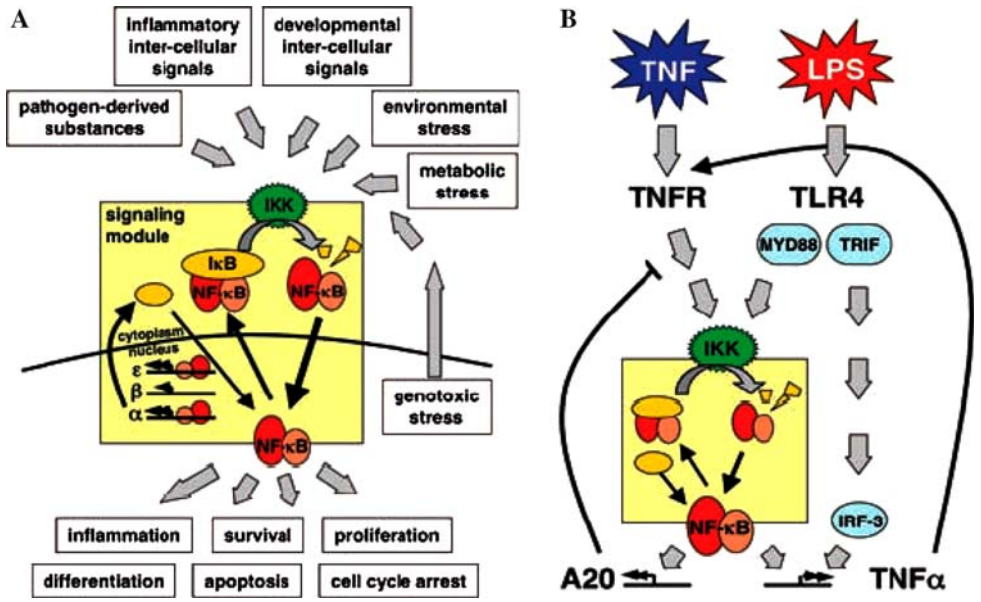

Fig. 4 Stimulation of NF-κB module by LPS, Werner et al. [43]. (**a**) The schematic illustrates the core of IκB|NFκB signaling module: many physiological signals impinge on the signaling module to produce different physiological responses. (**b**) IKK activity is regulated by a signaling pathway—specific negative and positive feedback loops. The schematic shows the A20-mediated negative feedback loop in the TNFR signaling pathway, and a positive feedback/feedforward loop in the LPS signaling pathway that is controlled by NFκB and possibly by IRF3, resulting in the expression of TNFα. Both feedback mechanisms allow stimulus-specific temporal profiles of IKK activity, which result in stimulus-specific NFκB and gene expression patterns

efficiency is now proportional to the third power of NFκB concentration. Prolonged IKK activity results in prolonged NFκB nuclear localization, which peaks at about 70 min and then remain almost constant for the next 3 h. According to Covert et al. [44], the lack of oscillations in the case of LPS stimulation, is due to the fact that NFκB oscillatory module is stimulated through two separate pathways introducing two different time delays. The fast pathway involving MyD88 (myeloid differentiation primary response gene 88) results in IKK activation at 15 min, while the slower pathway involving Triff (TIR domain-containing adaptor inducing IFN-beta) is delayed by 30 min. This hypothesis is confirmed by experiments on wild-type, and then MyD88 or Triff deficient mouse embryonic fibroblast (MEF).

Recently the modified and expanded version of Hoffmann et al. [10] model was used to analyze NFκB induction at a broad range of TNFα doses. Following Lipniacki et al. [12] model, Cheong et al. [45] took into account the difference in nuclear and cytoplasmic volumes and included IKK activation with the rate proportional to the initial TNFα dose. They found that, in order to obtain the correct IKK activity profile, the rate of IKK activation must decrease in time. As we will see the same property is present in Lipniacki et al. [12] model, in which the activation coefficient remains constant but activation rate decreases due to depletion of the pool of neutral IKK.

Two-feedback Model: A20 Controls IKK Activity

The aim of the second model [12] was to highlight the role of the second negative feedback loop in NFκB regulation involving A20 which controls IKK activity. The idea was to simplify Hoffmann et al. model by approximating action of three IκB isoforms by IκBα—the single species from IκB family whose knockout is lethal [46], and which binds the majority of cytoplasmic NFκB, and then to analyze NFκB–A20–IKK feedback regulation by considering behavior of wild type and A20 knockout cells. Like IκBα, A20 is highly NFκB responsive and has a similar kinetics. By incorporating the second inhibitor, the model accurately predicts the profile of IKK activity for both wild type and A20 knockout cells under TNFα stimulation.

The model involves two-compartment kinetics of the activators IKK and NFκB, the inhibitors A20 and IκBα, and their complexes. It is assumed that the cytoplasmic complex IKK may exist in one of three forms:

- neutral (denoted by IKKn), synthesized ‘de novo’ and specific to resting cells without any extracellular stimulus such as TNFα or IL-1;
- active (denoted by IKKa), arising from IKKn upon TNFα or IL-1 stimulation;
- inactive, but different from the neutral form, arising from IKKa possibly due to overphosphorylation (denoted by IKKi).

In resting cells, the unphosphorylated IκBα binds to NFκB and sequesters it in an inactive form in the cytoplasm. In response to extracellular signals such as TNF, IKK is transformed from its neutral form (IKKn) into its active form (IKKa), capable of phosphorylating IκBα, leading to IκBα degradation. At the same time NFκB is activated by RelA phosphorylation [47]. Degradation of IκBα enables activated NFκB to enter the nucleus, where it rapidly upregulates the transcription of mRNAs of inhibitory proteins A20 and IκBα, as well as that of numerous other genes. The newly synthesized IκBα leads NFκB out of the nucleus and sequesters it in the cytoplasm, while A20 inhibits IKK by converting IKKa into the inactive form IKKi, a form different from IKKn, but also not capable of phosphorylating IκBα. Considering IKK, we assume that each form of IKK undergoes degradation with the same degradation rate, and that IKKa can form transient complexes with IκBα proteins or IκBα|NFκB complexes. Formation of these complexes leads to IκBα phosphorylation, ubiquitination, and degradation in the proteasome.

The inhibitor IκBα migrates between the nucleus and cytoplasm and forms complexes with IKKa and NFκB molecules. The nuclear IκBα|NFκB complexes quickly migrate into the cytoplasm. The second inhibitory protein A20 is considered only in the cytoplasm, where it triggers the inactivation of IKK. It is assumed that the transformation rate from IKKa into IKKi is a sum of a constant term and a term proportional to the amount of A20. The total amount of NFκB is kept constant, i.e., it is assumed that its degradation is balanced by synthesis, but the synthesis and degradation terms are omitted. For IKK, we have synthesis and degradation terms, but since all IKK forms degrade with the same degradation rate, after the equilibrium is reached, the total amount of IKK (i.e., IKKn + IKKa + IKKi) remains roughly constant.

Transduction Pathway: From Receptors to IKK Activation

Both models discussed do not analyze how the signal is transduced from the receptors to IKK. The original Hoffmann et al. [10] model simply assumes the IKK activity profile. In our model this profile (in the case of TNFα stimulation) results from the modeling of A20 feedback loop, but still the analysis of pathway between the TNFα receptors and IKK is missing. The first attempt to fill the gap between TNFα receptors and NFκB signaling module was made by Cho et al. [48] who proposed the model for TNFα mediated-signaling cascade leading to NFκB liberation (IκBα degradation) or to formation of a FADD complex and apoptosis. The signaling pathway involves activation of TNF receptor 1 (TNFR1) by TNFα and the formation of the TNFR1|TRADD|RIP|TRAF complex (TRADD = TNFR-associated death domain, RIP = receptor interacting protein, TRAF = TNF receptor-associated factor) in a series of enzymatic reactions. Then the receptor complex activates IKK, which in turn phosphorylates IκBα. Authors assume the classical scheme for enzymatic reaction

$$E + S \underset{k_2}{\overset{k_1}{\leftrightarrows}} ES \xrightarrow{k_3} E + P, \tag{13}$$

where E is an enzyme which combines with substrate S to form an enzyme–substrate complex with rate constant k_1. The process is reversible, and the complex may dissociate into E and S with rate constant k_2 or it may further proceed to form a product P with a rate constant k_3. The whole pathway is described by the system of 18 ordinary differential equations. Since the transition rates were not available, the proposed model is not realistic from the biological perspective; the assumed concentrations of substrates are of order of 20 μM, what seems too large. As a result all reactions proceed too fast and for example the peak of IKK activity happens after about 30 s, while in reality IKK activity reaches its maximum at about 10 min of TNFα stimulation. Nevertheless the model constitutes a step towards understanding of the TNFα mediated signaling pathway and clearly showed the transient nature of IKK activity.

Further developments of TNF-NF-κB signaling are due to Park et al. [13] who combined Hoffmann et al. [10] model and the model of transduction pathway proposed by Cho et al. [48] in a more comprehensive model consisting of 52 ODEs. The aim of the model was to analyze responses of HepG2 cells and HepG2.2.15 cells (HepG2 cells producing hepatitis B virus) to TNFα stimulation. Hepatitis B virus (HBV) infection induces sustained NFκB activation, in a manner similar to TNFα stimulation. However, the response to the virus and TNFα does not add up. In contrast, when HepG2.2.15 cells are stimulated by TNFα, their response (the magnitude of NFκB oscillation) is weaker then in the case of uninfected cell. This makes them more vulnerable to apoptosis ([48], Fig. 1).

The model offers the following explanation of this "paradox": the amplitude and period of NFκB oscillations do not depend on the absolute level of active IKK (IKKa), but rather on the change of this level. The drop of the IKKa level induces oscillations, but of the opposite phase. In HepG2 cells not producing HBV, the initial IKKa level is low and TNFα stimulation results in sharp rise of IKKa inducing NFκB oscillations with high amplitude. In HepG2.2.15 cells, according to experimental data, initial levels of IKKa and nuclear NFκB are substantially higher, thus one may expect a smaller change in IKKa level after the TNFα stimulation. In order to obtain initial levels of nuclear NFκB and IKKa in HepG2 and HepG2.2.15 cells in accordance with the experimental data, additional factors

X and Y are added to the model. This modification of initial conditions enables to obtain the high-amplitude oscillations for HepG2 and lower amplitude oscillations with shorter period for HepG2.2.15 cells.

Paradoxically, experiments show that the TNFα stimulation of HepG2.2.15 cells induces NFκB oscillations, which are in the opposite phase to the uninfected HepG2 cells. After the TNFα stimulation the level of active NFκB first decreases then grows. In order to simulate this undershot effect, a further modification to the model is introduced. Namely it is assumed that in HepG2.2.15 cells TRAF is inhibited by phosphorylated form of NIK which attenuates IKKK and the IKK activity.

The strongest discrepancy between Park et al. [13] and Lipniacki et al. [12] is in the IKK activity profile. According to Lipniacki et al. model, IKK activity is transient, the high peak at about 10–15 min after the TNFα stimulation is followed by a very low tail. In the case of A20-deficient cells the tail is higher, but still much lower then the peak. Elevated tail prevents the IκBα resynthesis and the NFκB oscillations, as shown by the model and Lee et al. [7] experiments. Once NFκB enters the nucleus, it remains there at very high level. The transient character of IKK activity was observed first by Delhase et al. [49] in HeLa cells and then by Lee et al. [7] in mouse fibroblasts, and then by Werner et al. [43]. This transient nature of IKK activity is possibly due not to the phosphatase dephosphorylation but rather, as shown by Delhase et al. [49] to overphosphorylation.

Stochastic Models

Stochastic Version of the NFκB Model

In this model [50], transcriptional regulation of A20 and IκBα genes is governed by the rapid coupling between NFκB binding and transcription. In this situation, stalled RNA polymerase II is rapidly activated by NFκB binding to enter a functional elongation mode, and requires continued NFκB binding for reinitiation. This is represented in the model by tight coupling of NFκB binding to mRNA transcription. In fact, the experimental analysis of the kinetics of IκBα and A20 gene expression indicates that the patterns of mRNA expression are tightly coupled with NFκB presence in the nucleus, without appreciable time delay [51]. This model cannot be extended to other NFκB dependent genes that show distinct kinetics of induction. In this situation, the so-called "late" genes, like Naf-1 (Nef-associated factor 1) or NFκB2 show a peak of induction 6 h after NFκB binding. Activation of the late genes apparently requires the activation or binding of other rate-limiting regulatory factors [52]. Let us assume that all cells are diploid, and both A20 and IκBα genes have two potentially active homologous copies, each of them independently activated due to binding of NFκB molecule to specific regulatory site in gene promoter. Following [14, 21, 24, 26, 28, 53], we made the simplifying assumption that each gene copy may exist only in two states; active and inactive. When the copy is active the transcription is initiated, when the copy is inactive, transcription stops. The gene copy is inactivated when NFκB molecule is removed from its regulatory site due to the action of IκBα molecules, which bind to DNA-associated NFκB, exporting it out from the nucleus.

The most important is the single assumption that transcription of A20 and IκBα genes turns on and off with probabilities determined by regulatory factors. This distinguishes the applied approach from the deterministic one in which the transcription speed is a function of concentrations of these factors.

We split the reaction channels into fast and slow. We consider all reactions involving mRNA and protein molecules as fast and the reactions of gene activation and inactivation as slow. Fast reaction are approximated by the deterministic reaction-rate equations.

According to the above, the mathematical representation of the model [50] consists of 14 ordinary differential equations (ODEs) accounting for:

- formation of complexes and their degradation;
- transport between nucleus and cytoplasm; and
- transcription and translation;

and of four algebraic equations expressing the propensity functions of binding and dissociation of NFκB molecules to regulatory sites in A20 and IκBα promoters. Let us assume that both A20 and IκBα genes have two homologous copies independently activated due to NFκB binding. It is assumed that in an infinitesimal time interval Δt, the probability P^b of NFκB binding to regulatory sites in each allele is proportional to the nuclear amount of NFκB,

$$P^b(t, \Delta t) = \Delta t \times q_1 \times NF\kappa B_n(t). \tag{14}$$

NFκB dissociation probability, P^d, is a sum of a constant term and a term proportional to nuclear concentration of IκBα, which is capable of removing NFκB from regulatory sites in both A20 and IκBα genes,

$$P^d(t, \Delta t) = \Delta t \times (q_0 + q_2 \times I\kappa B\alpha_n(t)). \tag{15}$$

It is assumed that NFκB binding and dissociation are independent in homologous gene copies and that binding and dissociation propensities $r^b(t) = P^b(t, \Delta t)/\Delta t$ and $r^d(t) = P^d(t, \Delta t)/\Delta t$ are equal for each copy. The state of gene copy G^i (i = 1,2) is G^i = 1 whenever NFκB is bound to the promoter regulatory site, and G^i = 0 when the site is

unoccupied. As a result the gene state $G = G^1 + G^2$ can be equal to 0, 1 or 2. In this approximation the stochasticity of single cell kinetics solely results from discrete regulation of transcription of A20 and IκBα genes.

Let us assume that the transcription rate T_{rate} is

$$T_{\text{rate}} = c_2 + c_1 \times (G^1 + G^2). \quad (16)$$

Note that Eq. 16 naturally produces saturation in transcription speed. When the nuclear amount of regulatory factor NFκB is very large, then the binding probability is much larger than the dissociation probability, and the gene state will be $G = 2$ for most of the time. In such case the transcription will proceed at a maximum rate, $c_2 + 2c_1$. This rate has been measured for β-actin by single RNA transcript visualization as four mRNA molecules per minute per one allele [53]. In our calculations, we assumed $c_1 = 0.075$ mRNA/s, which corresponds to 4.5 mRNA molecules per minute. It is worth noting that the protein production rate is proportional to the product of transcription and translation efficiencies. Therefore, having solely information about the amount of protein one may not determine these two coefficients. When fitting the model, it was found that even if $c_2 = 0$, transcription is regulated satisfactorily, and therefore to minimize the number of free parameters we assume $c_2 = 0$. For the same reason it was assumed that $q_0 = 0$ in Eq. 15.

In model computations, the amounts of all the substrates are specified as the molecule counts. Since the ODEs are used to describe most of the model kinetics, amounts of molecules are not integer numbers, but since these numbers are in most cases much greater than 1, such description is reasonable. The implemented numerical scheme follows that of Haseltine and Rawlings [2].

Stochasticity of the model implies that simulations performed with the same model parameters and the same initial conditions, are different. Since each simulation corresponds to the evolution in a single cell, therefore, only the outcome averaged over many simulations corresponds to experimental data obtained for a population of cells in culture. As it can be seen in [50], with parameters fitted, the proposed model is able to faithfully reproduce time behavior of all variables for which the data is available: nuclear NFκB, cytoplasmic IκBα, A20 and IκBα mRNA transcripts, total IKK and IKK kinase catalytic activity (IKKa) in both wild-type and A20-deficient cells.

The model was fitted based on the experimental data from Lee et al. [7] and Hoffmann et al. [10] experiments on wild type and A20-deficient mouse fibroblast cells. We discuss briefly the main results coming from the model.

Let us focus first on resting cell regulation ([50], Fig. 2). In the absence of TNFα signal IKK remains in its neutral (inactive) form IKKn. This implies that it may not phosphorylate IκBα, which in turn degrades at a relatively slow rate due to "natural" degradation. Until the amount of IκBα exceeds that of NFκB, which is assumed to be constant, equal to 60,000 molecules, all NFκB remains in cytoplasmic complexes with IκBα. When due to natural degradation the amount of IκBα falls below 60,000, some NFκB (typically small fraction of cytoplasmic protein) enters the nucleus, where it may bind in a stochastic way to regulatory sites of IκBα and A20 promoters. Binding to IκBα results in a burst of IκBα transcription followed by an increase in IκBα protein level. In turn, free IκBα enters the nucleus, takes NFκB out of its regulatory site and leads almost all NFκB back into the cytoplasm. Binding to A20 promoter results in a burst of A20 transcription, but A20 may not terminate the NFκB binding. As a result, each time NFκB enters the nucleus it causes a burst of IκBα, but not necessarily of A20. Let us note that since all cells in the population (in absence of external signal like TNF) behave asynchronously, the average IκBα and A20 transcript and protein levels in the cell population remain constant (plot not shown). The relatively low transcript level observed for IκBα and A20 in the population of unstimulated cells is usually explained by the existence of some basal transcription, independent to NFκB. However, our model shows that, even if the basal transcription rate is zero, the average IκBα and A20 mRNA levels may be positive and constant in time for unstimulated cells.

In Fig. 5, we show the time behavior of the main variables of the single cell simulation together with the average over population of 500 cells. The simulation was performed for wild-type cells, in which all genes were potentially active. At $t = 1$ h, the rectangular TNFα signal is turned on for 6 h, i.e., until the end of the simulation time. Under the TNFα signal, IKK is promptly transformed into the active state IKKa and then into the inactive state IKKi. As a result, the persistent TNFα stimulation causes a pulse activation of IKK, followed by a low tail. The pulse of IKKa initiates the cascade. First, the free cytoplasmic IκBα and cytoplasmic complexes (IκBα|NFκB) are degraded (Fig. 5b). The released NFκB builds up in the nucleus, where it binds in a stochastic way to the regulatory sites in IκBα and A20 promoters (Fig. 5d, e). Let us assume the same binding and dissociation probabilities for the IκBα and A20 genes. However, due to stochasticity, their activity in a single run may be considerably different, although in general it coincides with high nuclear levels of NFκB. Due to the discrete regulation of trancriptional efficiency, the IκBα and A20 transcript levels (Fig. 5f, g) look saw-like, with kinks corresponding to binding and dissociation events. The newly synthesized IκBα enters the nucleus and leads almost all NFκB out of it (Fig. 5c), while A20 (Fig. 5h) triggers IKK inactivation. Let us note that since some NFκB molecules are present in the nucleus

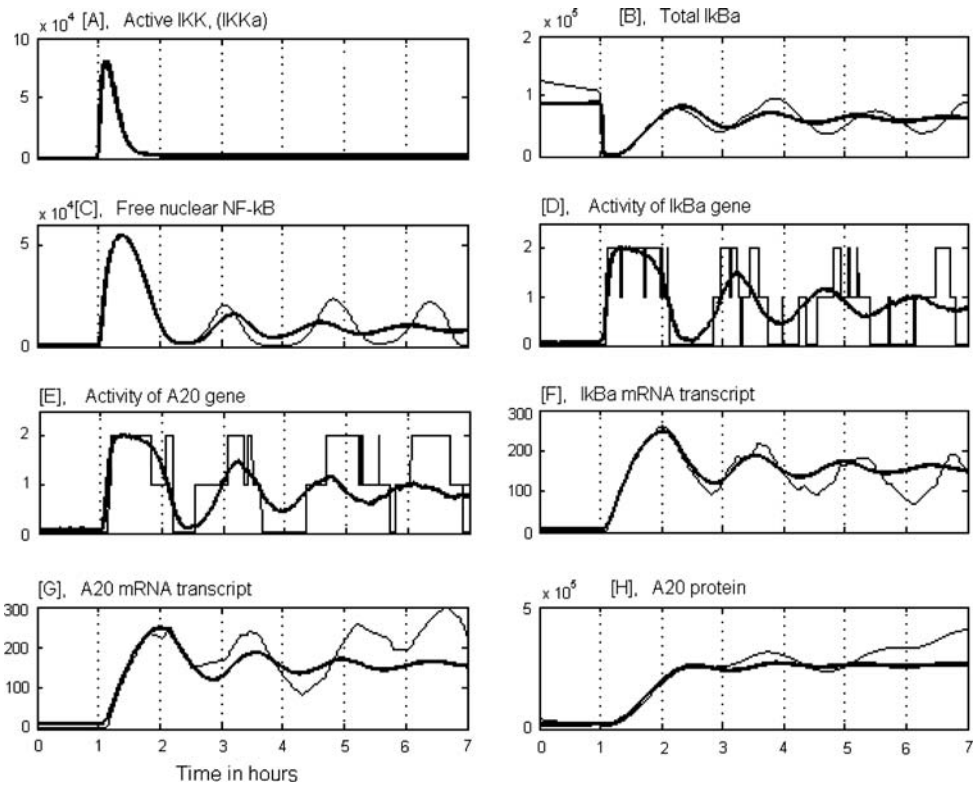

Fig. 5 Numerical solutions of Lipniacki et al. [50] stochastic model corresponding to a single wild-type cell (*thin line*) and the average over 500 simulations (*bold line*). Persistent TNF α activation starts at an hour. Panels (**a**) to (**h**) the amounts of selected substrates are expressed in numbers of molecules

even in the absence of TNFα stimulation and may bind to regulatory sites, the system (single cell) does not have a steady state, neither in the absence nor in the presence of the TNFα stimulation. The averaged kinetics is considerably different from kinetics of any particular cell. Despite the fact that each cell oscillates under extended TNFα stimulation, all quantities averaged over many cells converge to steady state levels. This effect is caused by a growing desynchronization of cells. Prior to the TNFα signal the cells are desynchronized (the single cell simulations are started at 20–30 h prior to TNFα signal), it is the TNFα signal that induces cell synchronization. The sharp decrease in total IκBα, followed by build up of nuclear NFκB is observed in all simulations (Fig. 6). Thereafter the stochastic nature of NFκB binding causes that the peaks of gene activity do not match, and this desynchronizes cell kinetics. The activity of the IκBα and A20 genes, averaged over a relatively large population, corresponds to the nuclear NFκB level much better than it does in the singe cell case.

In Fig. 6, we compare oscillations in nuclear NFκB level predicted by the model, with those measured in

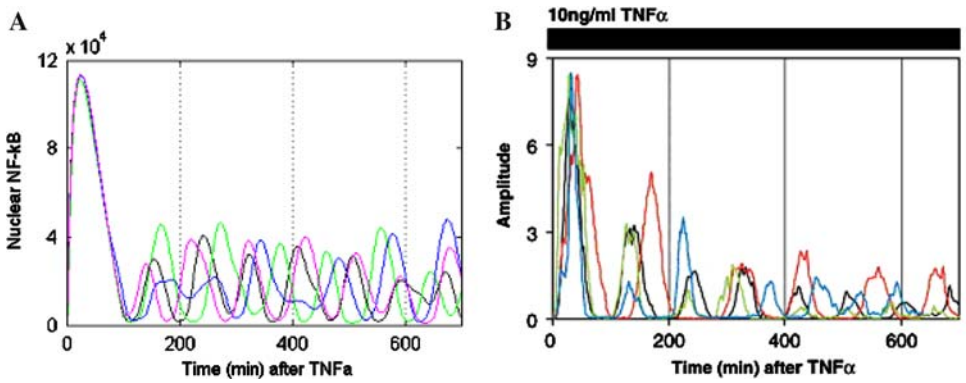

Fig. 6 Lipniacki et al. [50] model simulations, and measurements of Nelson et al. [35]. Four single-cell simulations or experiments are represented by different lines. (**a**) Model simulations. Nuclear NFκB following a persistent TNFα activation starting at $t = 0$. The total amount of NFκB was elevated to 120,000 for this simulation. (**b**) Nuclear to cytoplasmic RelA-DsRed fluorescence normalized to the highest peak intensity. Cells were treated with continuous 10 ng/ml TNFα

single-cell experiments by Nelson et al. [35]. Since the model was fitted based on data [7, 10] collected in experiments on mouse embryonic fibroblast, while Nelson et al. [35] did their experiments on SK-N-AS (human S-type neuroblastoma) cells only a qualitative comparison is possible. The cells analyzed were transfected with plasmids expressing RelA fused to the red fluorescent protein (RelA-DsRed). As reported, 91% of these control cells showed prolonged oscillations in RelA nuclear–cytoplasmic localization (N–C oscillations). These oscillations appeared quite synchronous between cells in the first few cycles, but than they became out of phase what explains why they appear to be strongly damped when observed at the population level (Fig. 8). In this simulation the level of total NFκB was elevated two times (with respect to the value measured by Carlotti et al. for fibroblasts [36, 54]) to 120,000 in order to mimic transfection. Nelson et al. [55], estimated that the average overexpression of RelA fusion protein was 3–5 times that of endogenous RelA level. We found that the persistence, amplitude, and period of these oscillations is not very sensitive to the total amount of total NFκB molecules. In Fig. 7, we compare the model

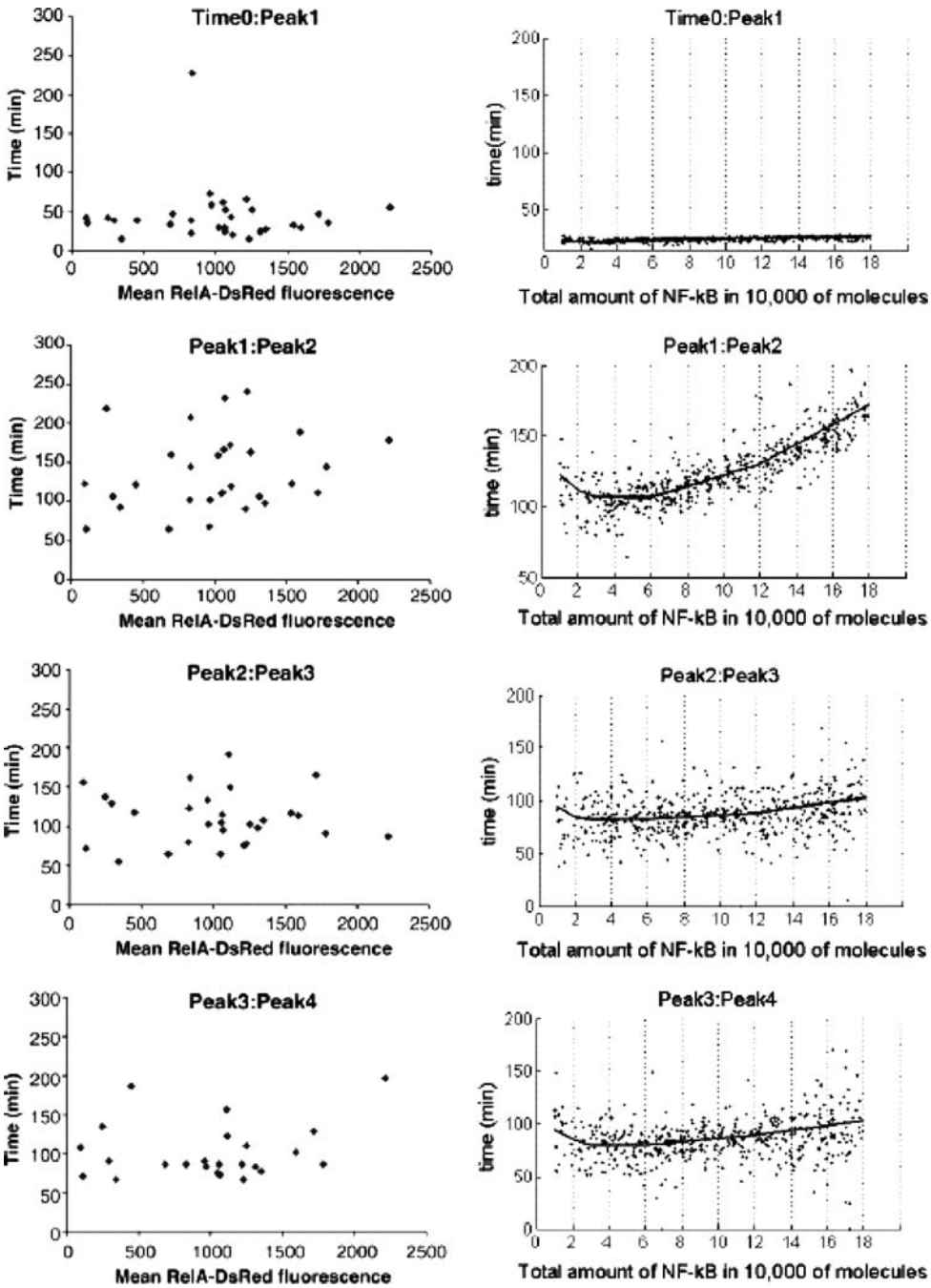

Fig. 7 Correlation of the total NFκB level with the peak-to-peak timing of NFκB oscillations. *Left column:* Nelson et al. [55], experiment on SK-N-As cells. *Right column:* Model predictions. The line represents the average calculated based on 100 simulations performed at each point corresponding to the total amount of NFκB equal to 10,000, 20,000, 30,000, 60,000, 120,000, and 180,000 molecules. The dots corresponds to 500 single simulations, each performed for the amount of total NFκB randomly selected from distribution uniform on (10,000, 180,000)

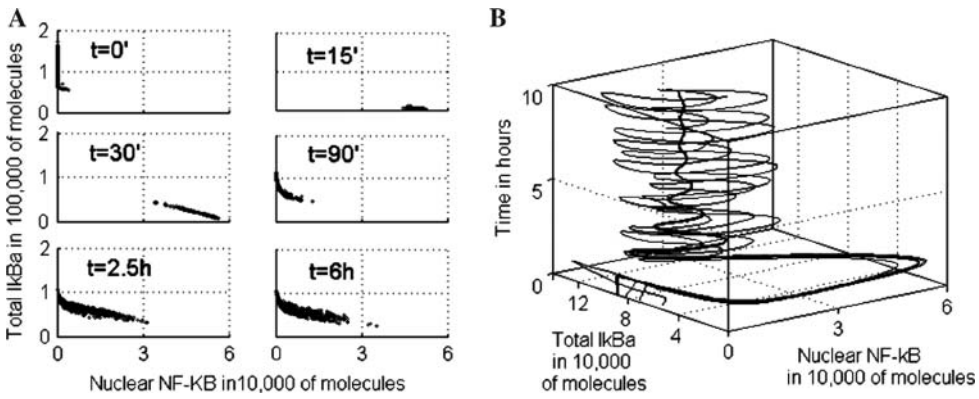

Fig. 8 Stochasticity in NF-κB signaling. (**a**) Scatter plots of total IκBα versus nuclear NF-κB at six times after start of TNF stimulation. (**b**) Trajectories projected on the hyperplane of total IκBα, nuclear NFκB, and time. *Thin lines* denote three single cell trajectories, while the *bold line* denotes the averaged trajectory

prediction of the correlation of the peak-to-peak timing with the NFκB level to the data of Nelson et al. ([35], Fig. 1) where, there is little or no correlation between the RelA-DsRed expression level and subsequent peak timing for SK-N-AS cells. According to the model, the 18-fold increase in total NFκB causes about 1.6-fold change in first-to-second peak timing, but less than 20% change in subsequent peak timing. Similarly timing of the first peak is not sensitive to the level of NFκB (Fig. 7).

Recently there was an interesting discussion between Barken et al. [56], and Nelson et al. [55], concerning the dependence of oscillation period and oscillation persistence to the amount of NFκB. Barken et al. [56], based on the Hoffman et al. [10] model showed that oscillation period strongly depends on the assumed amount of total NFκB, concluding that oscillations recorded in the overexpressed feedback system do not allow one to conclude that oscillations of the same persistence, amplitude, and period occur in normal genetically unaltered cells. In fact, according to the Hoffman et al. model [10], the 4-fold NFκB overexpression causes that the second peak in nuclear NFκB to appear not at 2 h (as normally) but at 5.5 h of persistent TNFα stimulation ([56], Fig. 1a). Even the relatively small 1.5-fold NFκB overexpression causes substantial alternations in the NFκB nuclear profile. This prediction is not confirmed by experiment ([55], Fig. 1). Following Nelson et al. [55], we expect that the substantial delay of the second peak associated with the elevation of total NFκB level is due to the Hoffmann et al. [10] assumption that the inducible IκBα expression is a second order polynomial in nuclear NFκB. As a result the 4-fold change in NFκB level causes a 16-fold increase in IκBα expression, which becomes so abundant that it would inhibit NFκB nuclear re-entry for about 5 h. Such large increase in IκBα expression seems to us to be biologically unjustified: there is a maximal physiological expression efficiency, which cannot be exceeded even if the regulatory factor is fairly abundant. Our current model shows that even the normal amount of NFκB is capable of turning IκBα gene on (Fig. 5) for about 1/2 h during the first pulse, which implies that further growth of NFκB nuclear level does not cause a significant rise in IκBα expression. Equation 16 in our model provides the natural saturation in transcription speed, but even the simple modification in which the second order polynomial is replaced by a linear term results in reduced sensitivity of period to the NFκB concentration ([12], Fig. 9) and ([55], Fig. 2).

Finally, let us also note that the oscillations predicted by any of the deterministic models [10, 12, 55] have essentially a different character than those in single cells, as shown in Fig. 6b. Oscillation amplitude in deterministic models decreases exponentially to zero, or some positive value with time, as opposed to the single-cell oscillations for which the amplitude is not a monotonous function of the peak number. For example in Fig. 6b, one can observe that the third peak of one of trajectories is higher than the second one, and that fourth peak of the other trajectory is higher than the third one. In ([35], Fig. 2a), the peak amplitude of red trajectory is growing starting from the second peak, and the green trajectory has third and fourth peaks higher than the second one. In the latter case the fluctuations in peak amplitude can be also due to the different kinetics of IκBα-EGFP and of endogenous IκBα.

One may visualize the cell-to-cell variability by the scatter plots showing, for example, the relationship between nuclear NFκB and its primary inhibitor IκBα, Fig. 8a. In resting cells, $t = 0$, there is almost no nuclear NFκB, which is sequestered by IκBα in the cytoplasm. In most of cells, the amount of total IκBα molecules is larger than the amount of total NFκB molecules, which is kept constant, equal to 60,000, during the time course of the simulation. At $t = 15$ min and 30 min, almost all IκBα is degraded and most of NFκB is present in the nucleus. Then at 90 min, IκBα rebuilds and again leads most of the NFκB out of the nucleus. Finally, 6 h after the beginning of TNFα stimulation the cell population is at apparent equilibrium, characterized by a relatively broad distribution of NFκB

and IκBα levels, an effect caused by desynchronization of the cell population. Despite the fact that the scatter plots in Fig. 8a, reveal that variability among cells grows in time, one may expect that there is a sizable fraction of cells the evolution of which is close to the averaged evolution. If fact, however, none of the cells behaves like the average, as shown in Fig. 8b single-cell trajectories keep oscillating although the steady state distribution is approached, and the average trajectory resulting from averaging over 500 simulated cells stabilizes.

Direct Stochastic Stimulation of Hoffmann Model: Magnitudes of Various Noise Sources

In order to estimate magnitudes of the potential contributions to cell-to-cell variability Hayot and Jayaprakash [57] performed direct simulations of few variants of simplified Hoffmann et al. [10] model. In all considerations the IκBβ and IκBε proteins are neglected.

Assuming that IBα transcription rate is linear as a function of the amount of NFκB, the IκBα protein results from following reactions

$$NF\kappa B_n \xrightarrow{tr_2} NF\kappa B_n + I\kappa B\alpha_t, \tag{17}$$

$$I\kappa B\alpha_t \xrightarrow{tr_1} I\kappa B\alpha_t + I\kappa B\alpha. \tag{18}$$

The first reaction describes production of IκBα transcript from nuclear NFκB (with propensity tr_2), the second one synthesis of IκBα protein from IκBα transcript (with propensity tr_1). In this expression model the fluctuations in gene activity are neglected, or are considered to be fast enough to assume that average gene activity is proportional to the amount of the NFκB. It is shown that for transcription and translation rates $tr_2 = 0.0582\ \text{min}^{-1}$ and $tr_1 = 0.2448\ \text{min}^{-1}$, corresponding to the original values of Hoffmann model 2002 the transcription noise is negligible and the cell-to-cell variability is low. As show by Thatai and Oudenarden [17], Kierzek [16], and Raser with O'Shea [24] the noise grows with decreasing transcription speed. After decreasing transcription rate 10 times and increasing translation rate 10 times (to keep the average protein production unchanged) the cell-to-cell variability was substantially increased ([57], Fig. 2 versus Fig. 1 h–j). The point is very interesting since the inducible transcription rate in Hoffmann model [10] was overestimated, and recently based on biological considerations was decreased by the authors almost four order of magnitude [12, 45]. This implies that the transcription noise, and thus the cell-to-cell variability can be even higher.

The next step is to consider the fluctuations in IκBα gene activity. Now, the reactions considered are the following

$$DNA + NF\kappa B \xrightarrow{k_b} DNA^*,\ DNA^* \xrightarrow{k_f} DNA + NF\kappa B, \tag{19}$$

$$DNA^* \xrightarrow{tr_2} DNA + NF\kappa B + I\kappa B\alpha_t, \tag{20}$$

$$I\kappa B\alpha_t \xrightarrow{tr_1} I\kappa B\alpha_t + I\kappa B\alpha, \tag{21}$$

where DNA* denotes active DNA, (with NFκB molecule bound). The main difference with respect to Lipniacki et al. [50] transcription model is that these latter authors assume that gene inactivation is due to binding of IκBα molecules, which pull NFκB out of DNA. In Hayot and Jayaprakash model NFκB dissociated at every synthesis of IκBα mRNA. The difference is crucial since in [50] the single binding of NFκB can result in transcription of many IκBα mRNA molecules while in Hayot and Jayaprakash [57] model it always results in production of a single transcript molecule. When NFκB binding occurs rapidly ($k_b = 1{,}200\ \text{min}^{-1}$), then the transcription is the limiting step, and the output is very similar to the previous model in which the fluctuations in gene activity were neglected. However, when binding is slow ($k_b = 12\ \text{min}^{-1}$), and compensated by 200 times higher translation rate then the cell-to-cell variability is larger than in the previous model ([57], Figs. 4, 5). In fact since NFκB binding results only in production of one IκBα molecule, the assumption that the promoter binding is weak is almost equivalent to the lowering of the transcription rate. This explains why the observed variability is still smaller than in our model in which the fluctuations in gene activity lead to burst of mRNA molecules.

Hayot and Jayaprakash [57] consider also the extrinsic noise due to both variability in total amount of NFκB molecules and initial amount of active IKK molecules. They found that when the initial distribution of active IKK is Gaussian with mean 30,000 and standard deviation 5,000 then the trajectories averaged over many cells (1,000 in simulations) exhibit damped oscillations. Again, the damping is not a property of any single cell but results of averaging over population of cells which exhibit less and less synchronized oscillations.

Conclusions and Perspectives

As a result of work of several groups of experimentalists and theoreticians, we have now a good quantitative understanding of some aspects of the core module of the NFκB pathway. Activity of NFκB as a transcription factor is triggered by activated IKK kinase, and regulated by two negative feedback loops, which involve products of NFκB-dependent genes: first loop involves NFκB inhibitors IκBα and IκBε. Second loop involves A20 protein, which

attenuates IKK activity and in this way protects IκBα and IκBε from degradation. Dynamics of these feedbacks has been quantitatively modeled in a series of studies, starting from the seminal paper by Hoffmann et al. [10]. This model took into account only the first feedback loop. It was followed by Lipniacki et al. [12], in which the A20 loop was added and its role in attenuation of IKK activity was modeled using data on A20 knockout cells [7]. Further studies by Cho et al. [48] and Park et al. [13] addressed various aspects of the transduction pathway connecting TNFα receptors with NFκB module. The works by Covert et al. [44] and Werner et al. [43] comparing LPS and TNFα mediated responses proved that specific gene expression is governed by the temporal control of IKK activity. As shown by Covert et al. [44] LPS stimulation activates IKK by Trif and MyD88 mediated pathways, what results in a prolonged IKK activity and in turn in non-oscillatory behavior of the NFκB module.

Recently, White's laboratory in Liverpool and Qwarnstrom's laboratory in Shefield produced a range of single-cell measurements of dynamics of NFκB and IκBα under a variety of TNFα and IL-1 stimulation regimes [35, 37–39]. The persistent oscillatory trajectories were explained by stochastic gene transcription model in Lipniacki et al. [50], based on an approximation of the Gillespie algorithm. In subsequent work Hayot and Jayaprakash [57] estimated magnitudes of the potential contributions to cell-to-cell variability by performing direct stochastic simulations of simplified Hoffmann model.

As we perceive it, the role of modeling is to find missing elements in the mechanisms supposed and inferred from experiments by biologists. This is simply accomplished by running these incomplete models and demonstrating discrepancies with the experimental data. Then, a correction or addition may be proposed by the modelers, but the ultimate purpose is to suggest new experiments, the role of which is to uncover or to confirm the putative source of discrepancy. This process integrates the modeler in the loop, the iterations of which may lead to a more complete understanding of biology at the system level. This paradigm seems nicely illustrated by the NFκB modeling story: Hoffmann et al. [10] model was missing a plausible explanation for the IKK time change. This was proposed by Lipniacki et al. [12] in the form of the A20 loop. Next Werner et al. [43] analyzed IKK activity profile in the case of LPS stimulation and difference between TNFα and LPS mediated gene expression was related to the difference in IKK activity profiles. Subsequently, Nelson et al. [35] experiments demonstrated that oscillation damping at the population level seems inconsistent with the more persistent oscillations at the single-cell level. This was explained by the Lipniacki et al. [50] and Hayot and Jayaprakash [57] models, which documented the need for stochastic transcription regulation to understand individual-cell oscillations. All in all, our understanding of how NFκB is regulated has thoroughly changed.

However, there is a long list of processes, which are still puzzling for modelers: as an example, not much has been accomplished in modeling NFκB phosphorylation. It has been documented by group of Brasier and coworkers [4, 58] that various phosphorylation sites in NFκB may define different NFκB active forms, which potentially may regulate various group of genes. Understanding this mechanism may lead to a better explanation of different timing of transcription activation of different groups of NFκB-dependent genes [51, 52, 59]. Models of crosstalk with other pathways such as p53, RelB, heat shock protein, and of the proliferation/apoptosis switch, are still pending.

Last but not least, the role of stochasticity in NFκB regulation is still equivocal. Is stochasticity a "side effect" due to the low number of reacting molecules, such as gene copies, mRNAs, receptors or external activating molecules, or does it play a more distinctive role in the early immune response? Let us consider stochastic gene activation. According to the mechanism described, high level of the transcription factor assures activation of all NFκB dependent genes, whereas the low level of NFκB implies a lower probability of activation of any particular gene. As a result, some genes may become activated and some not. Let us notice, however, that only the probability of gene activation decreases with NFκB concentration, while the size of mRNA's burst is independent of the concentration.

Another example is provided by the low-dose experiments of Cheong et al. [45], and White (private communication). Such low-dose stimulation is important for analysis of cell-to-cell signaling—a first step toward building of tissue models. Cheong et al. [45] found that average cell response (measured as NFκB nuclear translocation) is a decreasing function of TNFα dose, across a very broad range of TNFα concentrations, from 10 to 0.01 ng/ml. The single-cell experiments performed by White's group (private communication) show that the individual cell responses also decrease with the dose, but in addition the fraction of cells that respond within a defined time period becomes smaller. The experiment suggests that at a very low dose, below 0.1 ng/ml, the single cell responses are almost dose-independent and only the fraction of responding cells decreases with dose. This may suggest that stochastic cell activation following such a low dose stimulation is caused by erratic receptor activation caused by the limited number of TNFα molecules.

Stochastic gene activation (leading to the burst of proteins) and stochastic cell activation (leading to the massive NFκB nuclear translocation) provides a specific "stochastic robustness" in cell regulation. If a given gene is activated, a large burst of proteins is produced, in order to assure a

sufficient level of activity of these proteins. Stochastic robustness assures the minimal response to the signal. Decreasing magnitude of the signal causes only lowering of the probability of response, which leads to a smaller fraction of responding cells. This can be a clever strategy: if the TNFα signal is low, some cells respond by a massive NFκB translocation, whereas some do not respond at all. It helps to avoid ambiguity, such as when a small nuclear concentration of NFκB lead to activation of an undefined fraction of NFκB responsive genes. It is natural to expect that such undefined response might do more harm than good. Thus a better strategy at the tissue level, with low signal, is to let some cells respond, and some cells ignore the signal. Stochastic robustness allows cells to respond differently to the same stimulation, but makes their individual responses better defined. Both effects could be crucial in early immune response: diversity in cell responses causes the tissue defense to be harder to overcome by relatively simple programs coded in viruses and other pathogens. The more focused single-cell responses help cells to decide their individual fates, such as apoptosis or proliferation.

Acknowledgments The authors would like to thank Drs. Allan R. Brasier and Michel R. H. White for discussion and Dr. Pawel Paszek for help with preparing figures. This work was supported by Polish Committee for Scientific Research Grants No. 4 T07A 001 30 and 3 T11A 019 29, and by NHLBI contract N01-HV-28184, Proteomic technologies in airway inflammation (A. Kurosky, P.I.)

References

1. Gillespie, D. T. (1977). Exact stochastic simulations of coupled chemical reactions. *The Journal of Physical Chemistry, 81*, 2340–2361.
2. Haseltine, E. L., & Rawlings, J. B. (2002). Approximate simulation of coupled fast and slow reactions for stochastic chemical kinetics. *The Journal of Chemical Physics, 117*, 6959–6969.
3. Brasier, A. R. (2006). The NF-κB regulatory networks. *Cardiovascular Toxicology, 6*, 111–130.
4. Hoffmann, A., & Baltimore, D. (2006). Circuitry of nuclear κB factor signaling. *Immunological Review, 210*, 171–186.
5. Sun, S.-C., Ganchi, P. A., Ballard, D. W., & Greene, W. C. (1993). NF-κB controls expression of inhibitor IκBα: Evidence for an inducible autoregulatory pathway. *Science, 259*, 1912–1915.
6. Krikos, A., Laherty, C. D., & Dixit, V. M. (1992). Transcriptional activation of the tumor necrosis factor alpha-inducible zinc finger protein, A20, is mediated by kappa B elements. *The Journal of Biological Chemistry, 267*, 17971–17976.
7. Lee, E. G., Boone, D. L., Chai, S., Libby, S. L., Chien, M., Lodolce, J. P., & Ma, A. (2000). Failure to regulate TNF-induced NF-κB and cell death responses in A20-deficient mice. *Science, 289*, 2350–2354.
8. Bauch, A., & Superti-Furga, G. (2006). Charting protein complexes, signaling pathways, and networks in the immune system. *Immunological Reviews, 210*, 187–207.
9. Karin, M. (1999). The beginning of the end: IκB kinase (IKK) and NF-κB activation. *The Journal of Biological Chemistry, 274*, 27339–27342.
10. Hoffmann, A., Levchenko, A. Scott, M. L., & Baltimore, D. (2002). The IκB – NF – κB signaling module: Temporal control and selective gene activation. *Science, 298*, 1241–1245.
11. Kearns, J. D., Basak, S., Werner, Sh. L., Huang, Ch. H., & Hoffmann, A. (2006). IκBε provides negative feedback to control NF-κB oscillations, signaling dynamics, and inflammatory gene expression. *The Journal of Cell Biology* DOI: 10.1083/jcb.200510155 JCB
12. Lipniacki, T., Paszek, P., Brasier, A. R., Luxon, B., & Kimmel, M. (2004). Mathematical model of NF-κB regulatory module. *Journal of Theoretical Biology, 228*, 195–215.
13. Park, S. G., Lee, T., Kang, H. Y., Park, K., Cho, K-H., & Jung, G. (2006). The influence of the signal dynamics of activated form of IKK on NFκB and anti-apoptotic gene expression: A systems biology approach. *FEBS Letters, 580*, 822–830.
14. Ko, M. S. H. (1991). Stochastic model for gene induction. *Journal of Theoretical Biology, 153*, 181–194.
15. McAdams, H. H., & Arkin, A. (1997). Stochastic mechanisms in gene expression. *Proceedings of the National Academy of Sciences USA, 94*, 814–819.
16. Kierzek, A. M., Zaim, J., & Zielenkiewicz, P. (2001). The effect of transcription and translation initiation frequencies on the stochastic fluctuations in prokaryotic gene expression. *The Journal of Biological Chemistry, 276*, 8165–8172.
17. Thattai, M., & Oudenaarden, A. (2001). Intrinsic noise in gene regulatory networks. *Proceedings of the National Academy of Sciences USA, 98*, 8614–8619.
18. Tomioka, R., Kimura, H., Kobayashi, T. J., & Aihara, K. (2004). Multivariate analysis of noise in genetic regulatory networks. *Journal of Theoretical Biology, 229*, 501–521.
19. Kærn, M., Elston, T. C., Blake, W. J., & Collins, J. J. (2005). Stochasticity in gene expression from theories to phenotypes. *Nature Reviews, 6*, 451–464.
20. Walters, M. C., Fiering, S., Eidemiller, J., Magis, W., Groudine, M., & Martin, D. I. K. (1995). Enhancers increase the probability but not the level of gene expression. *Proceedings of the National Academy of Sciences USA, 92*, 7125–7129.
21. Blake, W. J., Kærn, M., Cantor, C. R., & Collins, J. J. (2003). Noise in eucaryotic gene expression. *Nature, 422*, 633–637.
22. Takasuka, N., White, M. R. H., Wood, C. D., Robertson, W. R., & Davis, J. R. E. (1998). Dynamic changes in prolactin promoter activation in individual living lactotrophic cells. *Endocrinology, 139*, 1361–1368.
23. Stirland, J. A., Seymour, Z. C., Windeatt, S., Norris, A. J., Stanley, P., Castro, M. G., Loudon, A. S. I., White, M. R. H., & Davis, J. R. E. (2003). Real-time imaging of gene promoter activity using an adenoviral reporter construct demonstrates transcriptional dynamics in normal anterior pituary cells. *The Journal of Endocrinology 178*, 61–69.
24. Raser, J. M., & O'Shea, E. K. (2004). Control of stochasticity in eukaryotic gene expression. *Science, 304*, 1811–1814.
25. Elowitz, M. B., Levine, A. J., Siggia, E. D., & Swain, P. S. (2002). Stochastic gene expression in a single cell. *Science, 297*, 1183–1186.
26. Kepler, T. B., & Elston, T. C. (2001). Stochasticity in transcriptional regulation: Origins, consequences, and mathematical representations. *Biophysical Journal, 81*, 3116–3136.
27. Pirone, J. R., & Elston, T. C. (2004). Fluctuations in transcription factor binding can be explain the graded and binary responses observed in inducible gene expression. *Journal of Theoretical Biology, 226*, 111–121.
28. Lipniacki, T., Paszek, P., Marciniak-Czochra, A., Brasier, A. R., & Kimmel, M. (2006). Transcriptional stochasticity in gene expression. *Journal of Theoretical Biology, 238*, 348–367.
29. van Kampen, N. G. (1992). *Stochastic processes in chemistry and physics*. Amsterdam: North-Holland.

30. Cao, Y., Petzold, L. R., Rathinam, M., Gillespie, D. T. (2004). The numerical stability of leaping methods for stochastic simulation of chemically reacting systems. *The Journal of Chemical Physics, 121*, 12169–12178.
31. Gillespie, D. T. (2001). Approximate accelerated stochastic simulation of chemically reacting system. *The Journal of Physical Chemistry, 115*, 1716–1733.
32. Rao, Ch. V., Arkin, A. P. (2003). Stochastic chemical kinetics and the quasi-steady-state assumption: Application to the Gillespie algorithm. *The Journal of Chemical Physics, 118*, 4999–5010.
33. Cao, Y., Gillespie, D. T., & Petzold, L. R. (2005). The slow-scale stochastic algorithm. *The Journal of Chemical Physics, 122*, 014116.
34. Puchalka, J., & Kierzek, A. M., (2004). Bridging the gap between stochastic and deterministic regimes in the kinetic simulations of the biochemical reaction networks. *Biophysical Journal, 86*, 1357–1372.
35. Nelson, D. E., Ihekwaba, A. E. C., Elliot, M., Johnson, J. R., Gibney, C. A., Foreman, B. E., et al. (2004). Oscillations in NF-κB signaling control the dynamics of gene expression. *Science, 306*, 704–708.
36. Carlotti, F., Chapman, R., Dower, S. K., & Qwarnstrom, E. E. (1999). Activation of nuclear factor κB in single living cells. *The Journal of Biological Chemistry, 274*, 37941–37949.
37. Nelson, G., Paraoan, L., Spiller, D. G., Wilde, G. J. C., Browne, A. M., & Djali, P. K., et al. (2002). Multi-parameter analysis of the kinetics of NF-κB signalling and transcription in single living cells. *Journal of Cell Science, 115*, 1137–1148.
38. Yang, L., Ross, K., & Qwarnstrom, E. E. (2003). RelA Control of IκBα phosphorylation. *The Journal of Biological Chemistry, 278*, 30881–30888.
39. Schooley, K., Zhu, P., Dower, S. K., & Qwarnstrom, E. E. (2003). Regulation of nuclear translocation of nuclear factor-κB RelA: Evidence for complex dynamics at the single-cell level. *The Biochemical Journal, 369*, 331–339.
40. Mendes, P. (2001). Modeling large biological systems from functional genomic data: Parameter estimation. In H. Kitano (Ed.), *Foundations of systems biology* (pp. 163–181). MIT Press.
41. Mendes, P. (1993). GEPASI: A software package for modelling the dynamics, steady states and control of biochemical and other systems. *Computer Applications in the Biosciences, 9*, 563–571; Mendes, P. (1997). Biochemistry by numbers: Simulation of biochemical pathways with Gepasi 3. *Trends in Biochemical Sciences, 22*, 361–363; Mendes, P., & Kell, D. B. (1998). Non-linear optimization of biochemical pathways: Applications to metabolic engineering and parameter estimation. *Bioinformatics, 14*, 869–883.
42. Fujarewicz, K., Kimmel, M., Lipniacki, T., & Świerniak, A. (2007). Adjoint systems for models of cell signaling pathways and their application to parameter fitting. *IEEE/ACM Transactions on Computational Biology and Bioinformatics, 4*, 322–335.
43. Werner, Sh. L., Barken, D., Hoffmann, A. (2005). Stimulus specificity of gene expression programs determined by temporal control of IKK activity. *Science, 309*, 1857–1861.
44. Covert, M. W., Leung, Th. H., Gaston, J. E., & Baltimore, D. (2005). Achieving stability of lipopolysaccharide-induced NFκB activation. *Science, 309*, 1854–1857.
45. Cheong, R., Bergmann, A., Werner, Sh. L., Regal, J., Hoffmann, A., & Levchenko, A. (2006). Transient IκB kinase activity mediates temporal NFκB dynamics in response to wide rage of tumor necrosis factor-α doses. *The Journal of Biological Chemistry, 281*, 2945–2950.
46. Gerondakis, S., Grossmann, M., Nakamura, Y., Pohl, T., & Grumont, R. (1999). Genetic approaches in mice to understand Rel/ NF-κB and IκB function: Transgenics and knockouts. *Oncogene, 18*, 6888–6895.
47. Jiang, X., Takahashi, N., Matsui, N., Tetsuka, T., & Okamoto, T (2003). The NF-κB activation in lymphotoxin receptor signaling depends on the phosphorylation of p65 at serine 536. *The Journal of Biological Chemistry, 278*, 919–926.
48. Cho, K.-H., Shin, S.-Y., Lee, H.-W., & Wolkenhauer, O. (2003). Investigations into the analysis and modeling of the TNFα-mediated NFκB-signaling pathway. *Genome Research, 13*, 2413–2422.
49. Delhase, M., Hayakawa, M., Chen, Y., & Karin, M. (1999). Positive and negative regulation of IκB kinase activity through IKKβ subunit phosphorylation. *Science, 284*, 309–313.
50. Lipniacki, T., Paszek, P., Brasier, A. R., Luxon, B., & Kimmel. M. (2006). Stochastic regulations in early immune response. *The Biophysical Journal, 90*, 725–742.
51. Tian, B., Nowak, D. E., Jamaluddin, M., Wang, S., & Brasier, A. R. (2005). Identification of direct genomic targets downstream of the NF-kappa B transcription factor mediating TNFα signaling. *The Journal of Biological Chemistry, 280*, 17435–17448.
52. Paszek, P., Lipniacki, T., Brasier, A. R., Tian, B., Novak, D. E., & Kimmel, M. (2005). Stochastic effects of multiple regulators on expression profiles in Eukaryotes. *The Journal of Theoretical Biology, 233*, 423–433.
53. Femino, A. M, Fay, F. S., Fogarty, K., & Singer, R. H. (1998). Visualization of single RNA transcripts in situ. *Science, 280*, 585–590.
54. Carlotti, F, Dower, S. K., & Qwarnstrom, E. E. (2000). Dynamic shuttling of nuclear factor kappa B between the nucleus and cytoplasm as a consequence of inhibitor dissociation. *The Journal of biological chemistry, 275*, 41028–41034.
55. Nelson, D. E., Horton, C. A., See, V., Johnson, J. R., Nelson, G., Spiller, D. G., Kell D. B., & White, M. R. H. (2005). Response to comment on "Oscillations in NF-κB signaling control the dynamics of gene expression". *Science, 308*, 52b.
56. Barken, D., Wang, Ch. J., Kearns, J., Cheong, R., Hoffmann, A., & Levchenko, A. (2005). Comment on "Oscillations in NF-κB signaling control the dynamics of gene expression". *Science, 308*, 52a.
57. Hayot, F., & Jayaprakash, C. (2006). NFκB oscillations and cell-to-cell variability. *The Journal of Theoretical Biology, 240*, 583–591.
58. Jamaluddin, M., Wang, S., Boldogh, I., Tian, B., & Brasier, A. R. (2007). TNF-α-induced NF-κB/Rel A Ser (276) phosphorylation and enhance some formation on the IL-8 promoter is mediated by an ROS-dependent PKAc pathway. *Cellular Signalling, 19*, 1419–1433.
59. Tian, B., Nowak, D., & Brasier, A. R. (2005). A TNF induced gene expression program under oscillatory NF-κB control. *BMC Genomics, 6*, 137.